RSC Advances

PAPER

Cite this: *RSC Adv.*, 2018, **8**, 40454

Biocompatibility and photo-induced antibacterial activity of lignin-stabilized noble metal nanoparticles†

Diamela María Rocca,[ab] Julie P. Vanegas,‡[ac] Kelsey Fournier,‡[a] M. Cecilia Becerra,[b] Juan C. Scaiano[a] and Anabel E. Lanterna*[a]

Received 2nd October 2018
Accepted 25th November 2018

DOI: 10.1039/c8ra08169g

rsc.li/rsc-advances

One-pot thermal and photochemical syntheses of lignin-doped silver and gold nanoparticles were developed and their antimicrobial properties were studied against *Escherichia coli* and *Staphylococcus aureus*. The nature of the lignin as well as the metal are directly involved in the antimicrobial activity observed in these nanocomposites. Whereas one of the nanocomposites is innocuous under dark conditions and shows photoinduced activity only against *Staphylococcus aureus*, the rest of the lignin-coated silver nanoparticles studied show antimicrobial activity under dark and light conditions for both bacteria strains. Additionally, only photoinduced activity is observed for lignin-coated gold nanoparticles. Importantly, the particles are non-cytotoxic towards human cells at the bactericidal concentrations. Preliminary assays show these silver nanoparticles as potential antimicrobial agents towards *S. aureus* biofilm eradication.

Introduction

Threats posed by bacterial infections are of major public concern, leading to a boost in efforts to develop new antimicrobial agents.[1] The use of silver nanoparticles (AgNP) has been widely explored,[2–4] showing antimicrobial activity in the dark and under illumination.[5,6] Whereas some studies suggest silver nanoparticles are a simple source of silver ions,[7] a few years back our group demonstrated that the mechanism is more complex[8] and may involve direct action by the nanoparticles themselves. Gold nanoparticles (AuNP), also show antimicrobial activity. Although sometimes they are less effective, they can provide an alternative to silver based materials.[9] The use of metal nanoparticles for this type of application is directly related to the type of coating agents utilized to stabilize the particles in the biological media, while retaining the antimicrobial activity.[10] We have recently reported a one-pot synthesis of amoxicillin-coated gold nanoparticles that show synergistic antimicrobial activity upon light irradiation;[11] where the antimicrobial mechanism may involve the generation of localized heat and reactive oxygen species (ROS) upon light irradiation.[12,13] The growing interest in the use of environmentally friendly capping agents, as well as, the use of sustainable resources for antimicrobial applications,[14,15] such as food packaging,[16] has led our group towards the use of non-toxic and inexpensive capping agents.[17] Here we explore the use of lignin, the second most abundant natural polymer on earth after cellulose, as an alternative reducing and capping agent for the synthesis and stabilization of metal nanoparticles for potential applications as antimicrobial agents.

Lignin, a traditional low-value by-product of the pulp and paper industry, is gradually becoming a major output of the forestry industry, recognizing its rich chemical composition. There is growing interest in pursuing value-added applications for lignin, which traditionally has been regarded as waste and used for heat generation.[18] Due to its aromatic structure and the presence of multifunctional groups, lignin is believed to have potential applications as an additive in lubricants[19] or wood fuel pellets.[20] Other applications include the use of acid treated lignin nanoparticles for antimicrobial applications,[21] and heavy metal[22] or hydrogen peroxide[23] sensing. The term 'lignin' encompasses a wide range of chemical structures that even in nature vary depending on the type of species and the environment in which trees grow. But lignin is never extracted 'intact', as the mechanical, thermal and chemical treatments required for its extraction change its chemical composition, color and solubility. Chemical modifications can result in insoluble, water soluble and organo-soluble lignin. Therefore, the properties of

[a]*Department of Chemistry and Biomolecular Sciences and Centre for Advanced Materials Research (CAMaR), University of Ottawa, 10 Marie Curie, Ottawa, Ontario K1N 6N5, Canada. E-mail: alantern@uottawa.ca*

[b]*Departamento de Ciencias Farmacéuticas, Facultad de Ciencias Químicas, Universidad Nacional de Córdoba, Haya de la Torre S/N, Córdoba, X5000, Argentina*

[c]*Liquid Crystal Institute, Kent State University, 1425 Lefton Esplanade, Kent, OH 44242, USA*

† Electronic supplementary information (ESI) available: UV-Vis absorption spectra of different MNP@lignin nanocomposites studied, particle size distributions, UV-Vis spectra of the nanocomposites in different biological media and antibacterial activity of AuNP@lignin. See DOI: 10.1039/c8ra08169g

‡ Equal contribution.

the lignin are highly dependent on the conditions used during the process in which the lignin was extracted.[24] There is no such thing as the defined structure of lignin, but the main chemical features of pre-extracted lignin contains many substituted phenol groups, which are believed to be responsible for the antioxidant properties of lignin.[25,26] Furthermore, different types of lignin contain various levels of carbohydrates that are attached to the polymeric lignin moiety.[23,27] Beside its antioxidant properties, it has been proved that lignin can serve as a reducing agent in the mechanochemical synthesis of metal nanoparticles.[25] The use of silver-ion-infused lignin nanoparticles is an alternative to metallic AgNP in antimicrobial applications, although the former relies on the antimicrobial activity of silver ions.[8,28] Here we show lignin can act as reducing and capping agent during the one-pot synthesis of AgNP or AuNP. The new nanocomposites proved to be stable in biological media, demonstrate antimicrobial activity and be non-toxic for human cells at bactericidal concentrations.

Here we used three different types of lignin: commercially available alkali lignin (with low sulfonate content and no reducing sugars), ZHL lignin (depolymerized and 27% sugar content) and AL lignin (alkali-extracted, 16% sugar content) from a local pulp and paper company. Alkali lignin is soluble in water (pH $\sim$ 7) and ZHL and AL lignin are soluble in alkali solutions (pH $\sim$ 12), but insoluble under neutral and acidic conditions. It is important to highlight that whereas pH requirements are important for manufacturing the materials, their applications are studied at physiological pH. We show that colloidal lignin-coated AgNP and AuNP (AgNP@lignin or AuNP@lignin) can be synthesized in few minutes using thermal or photoinduced methodologies. Both, Ag and Au, show photoinduced antimicrobial activity, not only against Gram-negative (*Escherichia coli*) bacteria, but also against Gram-positive (*Staphylococcus aureus*) bacteria. Importantly, they show no cytotoxicity against human cells. Additionally, AgNP@lignin were tested for antimicrobial activity towards biofilms, which are highly resistant to antimicrobial agents as opposed to dispersed (planktonic) bacteria.[29]

Materials and methods

Chemicals

Tetrachloroauric acid-99% ($HAuCl_4 \cdot 3H_2O$), silver nitrate ($AgNO_3$), alkali lignin, Dulbecco's phosphate buffered saline (PBS), Luria Bertani (LB) broth, Dulbecco's Modified Eagle Medium (DMEM) Agar Mueller Hinton, trypsin, Fetal Bovine Serum (FBS), poly-L-lysine, 3-(4,5-dimethylthiazol-2-yl)-2,5-diphenyltetrazolium bromide (MTT), and 2,7-dichlorodihydrofluorescein diacetate ($DCFH_2$-DA) were purchased from Sigma-Aldrich, and used as received. AL and ZHL lignin were a generous gift from FP Innovations from Point-Claire, PQ, Canada.

Instrumentation

Centrifugations were carried out in an Eppendorf 5804R centrifuge equipped with a F-34-6-38 rotor. The UV-vis absorption spectra were recorded on an Agilent Cary 60 spectrophotometer. TEM images were recorded on a Jeol JEM-2100F transmission electron microscope (TEM) working at an accelerating voltage of 200 kV. The diameter of the nanoparticles was determined using ImageJ software. Statistical analysis was obtained by measuring the diameter of 200–400 nanoparticles per sample. Absorption and emission spectra for ROS and cell viability experiments were carried out in a 96 well-plate using a microplate reader SpectraMax M5. ζ-potential and dynamic light scattering (DLS) were measured with a Malvern Zetasizer (model Nano-S). The total amount of metal was determined by Inductively Coupled Plasma Optical Emission Spectrometry (ICP-OES), using an Agilent 5100 series ICP-OES equipment. Fourier Transform Infrared spectroscopy (FT-IR) was performed in a Nicolet 6700 FT-IR equipped with and attenuated total reflectance (ATR) accessory.

Synthesis and characterization of MNP@lignin

Colloidal lignin-coated metal NP (MNP@lignin) were prepared in a one-step synthesis using lignin as both the reducing and coating agent. Thermal and photochemical methodologies were used for the reduction of the metal precursor ($HAuCl_4$ or $AgNO_3$) with lignin (alkali, ZHL, or AL). Table S1† summarizes the conditions utilized for each synthesis. In general, 0.5 mL of the corresponding metal precursor solution was added to 0.5 mL of lignin (0.4 mg mL^{-1}) and the solution volume was increased to a final volume of 2 mL. For thermal synthesis, the solutions were heated up to 55–60 °C (Table S1†). Photochemical method was carried out by direct irradiation of the reaction mixture with 405, 465, 530 and 730 nm LEDs in accordance with Table S1.† The prepared colloidal samples were subjected to a centrifugation/washing cycle with MilliQ water in order to remove any unbound lignin moieties and/or unreacted metal precursor. Nanoparticles were resuspended in 200 μL of MilliQ water (stock solution), and after a 10× dilution they were characterized by UV-Vis spectroscopy, TEM, DLS and zeta (ζ)-potential. The total amount of metal (Ag or Au) was determined by ICP-OES. Briefly, triplicates of 10 mg of the solutions were accurately weighed and digested in 0.8 mL of aqua regia. After that, 5 mL of MQ water were added, and the solution was centrifuged at 7000 rpm for 10 minutes. The supernatants were then diluted to 10 mL prior measurement by ICP-OES. The nM concentration of the particles was calculated as described in the ESI.†[30]

Stability of MNP@lignin

The colloidal stability of MNP@lignin was determined in the three biological media. Briefly, 100 μL of the stock solution of NP was resuspended in 100 μL of different concentrations (100, 50, 37.5 and 25%) of PBS (pH 7), LB broth or DMEM and their plasmon absorption was monitored as a function of time during a period of 10 days.

Bacterial strains and growth conditions

The experiments were performed using *Staphylococcus aureus* 292S3 and *Escherichia coli* CF073. Stock cultures were

maintained in tryptone soya broth and stored at −80 °C in 10% glycerol.

Antimicrobial activity and ROS production

The Minimum Inhibitory Concentration (MIC) was determined by broth microdilution method, which was slightly modified from the standard Clinical and Laboratory Standards Institute (CLSI). In brief, an inoculum of 10^6 colony forming units (CFU) per mL was prepared from a single colony in LB broth containing different concentrations of solutions of AgNP@lignin, AuNP@lignin and $AgNO_3$. The absorbance was measured at 600 nm (OD_{600}) after 24 h of incubation at 37 °C under dark conditions. The MIC was determined as the lowest concentration of test compounds at which the absorbance of the bacterial inoculum at 600 nm was lower than 0.03.[8] All measurements were run in triplicate.

Antibacterial activity. Antibacterial activity of MNP@lignin was tested against *S. aureus* and *E. coli*. Bacterial suspensions of 10^6 CFU mL^{-1} in 50% LB from a single colony were prepared. Using a 96-well plate, 100 μL of bacterial suspension and 100 μL of the MNP@lignin solutions (at the given concentrations in 50% LB) were mixed and irradiated under different conditions (*vide infra*) at 37 °C. Control experiments were run under the same conditions in the dark. All samples were triplicated. Aliquots of each sample were diluted properly and seeded in Mueller Hinton agar plates. CFU were counted from the agar plates after 24 h of incubation at 37 °C.

ROS quantification in bacterial culture. The amount of ROS generated was determined using a reported protocol.[11,31] We utilized $DCFH_2$-DA as a prefluorescent probe to detect and quantify the total ROS generated by following the probe emission at 530 nm. Therefore, the radical indicators of oxidative stress were measured with $DCFH_2$-DA (2 μM) in bacterial suspensions (10^9 CFU mL^{-1}) treated with MNP@lignin at the given concentrations. The samples were irradiated with white light (Fig. S8†) for up to 1 h for AgNP@lignin and up to 6 h for AuNP@lignin.

Biocompatibility and cytotoxicity

The cytotoxicity and biofilm eradication experiments were carried out using MTT assay previously described.[32]

Cell viability. The 3T3 fibroblasts were cultured in Dulbecco's modified Eagle's medium (DMEM) with 10% calf serum. Cells were grown and attached in cells culture flasks using poly-L-lysine, and after that they were washed with phosphate-buffer saline and trypsinized with 1 mL of 0.05% trypsin. Trypsinization was stopped by adding fresh medium to the reaction. The cells were washed once by centrifugation with DMEM without serum, resuspended in medium without serum, and approximately 10^5 cells per well were plated after proper cell counting in an improved Neubauer chamber. They were incubated overnight to allow attachment and then treated with the bactericidal concentrations of AgNP@lignin and AuNP@lignin, lignin at 0.1 mg mL^{-1}, DMEM and irradiated with white light during 1 h in the case of AgNP@lignin nanocomposites and 6 h in the case of AuNP@lignin. In parallel dark conditions were tested. The cells were kept in that period of time at 37 °C, 5% CO_2, and 95% humidity. MTT assay based on the reduction of tetrazolium salt to formazan (absorbance at 570 nm) in living cells was done according to a Sigma protocol to determine the percent survival.

Biofilm formation. In order to form a strong biofilm, *S. aureus* were grown in LB broth supplemented with 0.25% glucose. After overnight incubation the well plate was rinsed with sterile PBS to remove planktonic bacteria before adding fresh LB media to the attached biofilm to carry out the eradication experiments.

Biofilm eradication. The mature biofilms formed in a 96-well plate were treated with AgNP@lignin nanocomposites at the bactericidal concentration. LB medium containing the AgNP@lignin composite (0.02 nM of AgNP@alkali, 2.9 nM of AgNP@AL or 9.8 nM Ag@ZHL) was added and incubated under white light or dark conditions for 3 h at 37 °C. Bacterial viability was determined using MTT essay following absorption at 570 nm. Briefly, the biofilms treated with AgNP@lignin or control (untreated) were washed once with PBS. A 250 μL aliquot of MTT solution (200 μg mL^{-1}) was added to each well and incubated in the dark for 3 h at 37 °C.

Table 1 Synthetic strategies used for each MNP@lignin composite[a]

MNP@lignin	Mass ratio (mg of metal precursor/mg of lignin)	Irradiation	T (°C)	t (min)
AuNP@alkali	0.5	532 nm	25	5
AuNP@ZHL	1	Dark	58	10
AuNP@AL	2	Dark	58	30
AgNP@alkali	5	465 nm	28	5
AgNP@ZHL	1	Dark	58	5
AgNP@AL	1	465 nm	28	5

[a] Conditions: 0.1 mg of lignin in water or pH 12 according to lignin solubility.

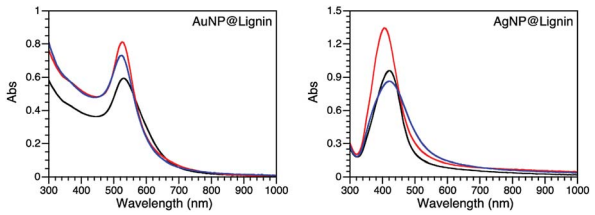

Fig. 1 Absorption spectra of the selected MNP@lignin synthesized with alkali (black), ZHL (red) and AL (blue) lignins following protocols described in Table 1.

Results

Synthesis and characterization of MNP@lignin

Different synthetic strategies were explored for Au and Ag NPs including thermal- and photo-chemical reactions utilizing the reducing properties of lignin. Table S1† summarizes all the conditions used for the synthesis optimization. After an extensive screening of conditions, each MNP@lignin was synthesized

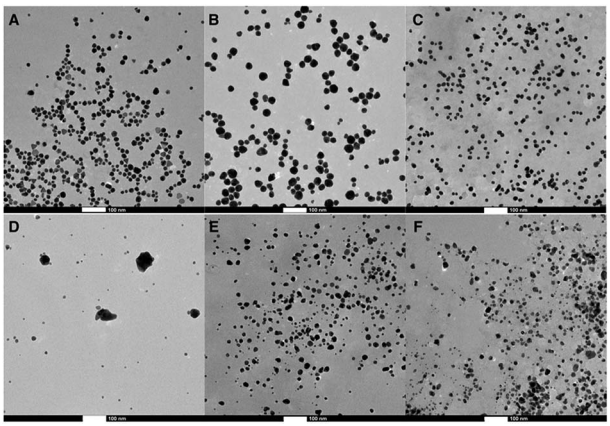

Fig. 2 TEM images of the MNP@lignin synthesized following protocols described in Table 1: (A) AuNP@alkali, (B) AuNP@ZHL, (C) AuNP@AL, (D) AgNP@alkali, (E) AgNP@ZHL, and (F) AgNP@AL. Scale bar: 100 nm.

by slightly modified conditions, which better suited the desired stability and optical properties of each NP. The most reproducible synthetic strategies are summarized in Table 1. Fig. 1 shows the absorption spectra of MNP obtained with different lignin sources and Fig. 2 and S2–S4† display the particle morphologies and sizes, respectively. Table 2 summarizes the particle size, hydrodynamic diameter and zeta(ζ)-potential for each batch of particles. It is important to highlight that all irradiation wavelengths tested furnished the formation of metal nanoparticles, possibly due to the capacity of lignin to thermally reduce Ag^{+} (or Au^{3+}) and the size and shape modulation upon irradiation.[33,34]

Stability in biological media

The stability of the particles in different biological media was determined by following the changes on their plasmon absorption band as function of time in each media. Particles were resuspended in different media concentrations (100, 50, 37.5 and 25%) and their stability over a period of 10 days was determined by eqn (1),[17] where 20% decrease in the plasmon absorption band was accepted as stability parameter. Fig. 3, S6 and S7† show the evolution of the plasmon band for media concentrations where particles were stable.

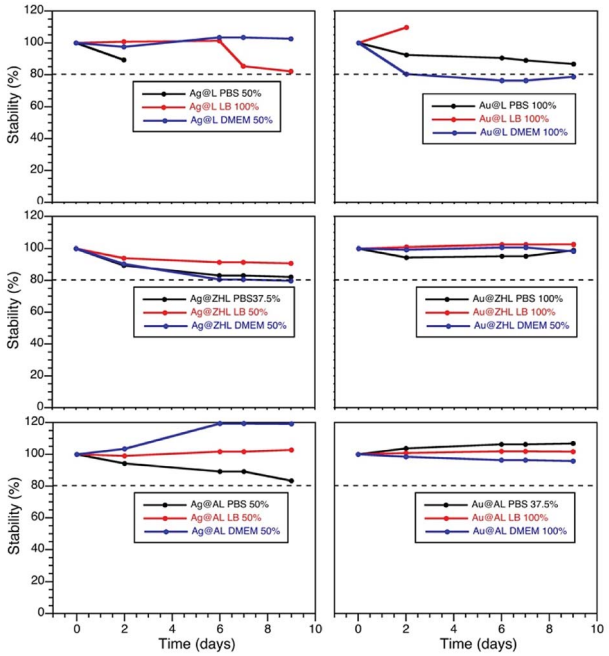

Fig. 3 Stability curves of AuNP@lignin and AgNP@lignin dispersed in different biological media. Data obtained from Fig. S5 and S6.†

$$\%\text{Stability} = \frac{\text{Abs}_{t_i}^{\max}}{\text{Abs}_{t_0}^{\max}} \times 100 \quad (1)$$

Fortunately, AgNP@lignin and AuNP@lignin show great stability at high media concentrations, which further suggest lignin as a strong stabilizing agent. After this, we selected LBB media to carry out the antibacterial activity experiments.

Antimicrobial activity

Analyzing the minimal inhibitory concentration (MIC) of MNP@lignin required under dark conditions, we were able to determine MIC values for AgNP@alkali and AgNP@AL of 0.2 μg mL^{-1} and 24.2 μg mL^{-1}, respectively. These numbers are significantly smaller than other reported.[36] Additionally, we show that the antimicrobial activity strongly depend on the type of lignin used. For instance, AgNP@ZHL nanocomposites show no bactericidal effect in the dark. As expected,

Table 2 Summary of the core size, hydrodynamic size and surface charge for each composite

MNP@lignin	Diameter[a] (nm)	Hydrodynamic diameter[b] (nm)	PDI	ζ-potential (mV)
AuNP@alkali	15 ± 7	39	0.42	−26.9
AuNP@ZHL	25 ± 8	39	0.27	−54.4
AuNP@AL	12 ± 4	21	0.65	−50.2
AgNP@alkali	8 ± 4[c]	65	0.52	−44.3
AgNP@ZHL	13 ± 8	52	0.28	−51.1
AgNP@AL	13 ± 6	100	0.67	−57.8

[a] From analyses of the TEM images. [b] From DLS analysis. [c] Only small particles were measured and considered. PDI: polydispersity index scaled between 0 and 1. Values higher than 0.7 indicate highly-polydisperse materials.[35]

AuNP@lignin are also innocuous under dark conditions. Nevertheless, we tested the antibacterial activity of all MNP@lignin nanocomposites under illumination utilizing the concentrations from Table S2.† Thus, low-density bacteria suspensions in LB broth ($\sim 10^6$ CFU mL^{-1}) were challenged at the composite concentrations shown in Table S2.† In order to differentiate between bactericidal and bacteriostatic activity, short-term (1 h for AgNP@lignin and 6 h for AuNP@lignin) time-killing studies were carried out with all MNP@lignin nanocomposites (Fig. 4 and S9†). It is important to note that alkali lignin alone shows no bactericidal activity. Additionally, ZHL and AL lignins are not soluble in biological media and therefore antimicrobial studies cannot be performed with these materials.

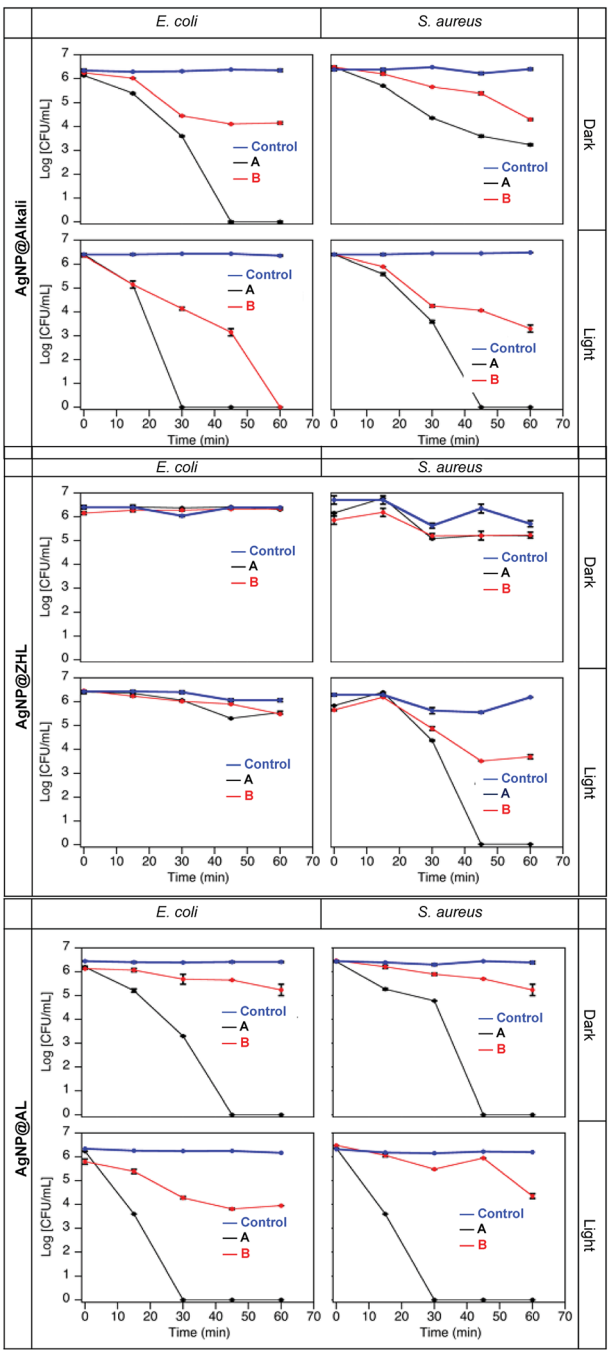

Fig. 4 Bacteria time-kill profiles for *E. coli* and *S. aureus* up to 1 h in the presence of AgNP@alkali, AgNP@ZHL, and AgNP@AL at A and B concentrations given in Table S2.† Control experiments were performed in the absence of nanocomposites.

ROS production

The production of ROS in the presence of bacteria was determined by a well-known protocol employing $DCFH_2$-DA.[37] This non-fluorescent probe undergoes deacetylation in the presence of bacteria esterase, which can be oxidized by the ROS species generated (see Fig. S10†) to furnish a highly fluorescent species. Thus, the total amount of ROS species generated is directly correlated to the emission detected at 530 nm (λ_{ex} 428 nm). Two different concentrations of MNP@lignin were used (A and B, see Table S2†) and the mixtures were irradiated with white light at ~ 78 Wm^{-2} during a 6 h period in the case of AuNP@lignin and 1 h period for AgNP@lignin. Fig. 5 summarizes the ROS species generated from AgNP@lignin nanocomposites and Fig. S11† shows the results obtained with AuNP@lignin nanocomposites.

Cell viability

The toxicity of the MNP@lignin nanocomposites towards mammalian cells was studied at the bactericidal concentrations with 3T3 fibroblasts, upon white light irradiation. Results shown in Fig. 6 suggest that all the MNP@lignin nanocomposites can be considered non-cytotoxic, with the exception of AgNP@alkali, which shows the same toxicity found with $AgNO_3$, whereas $HAuCl_4$ was considered non-toxic.[38] It is important to notice that the light dose used does not damage the cells. Also, it is important to highlight that only alkali lignin

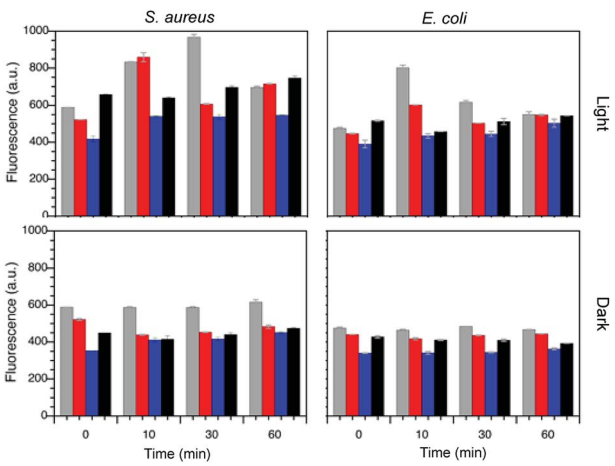

Fig. 5 ROS production for samples of *S. aureus* and *E. coli* in the presence of AgNP@alkali (grey), AgNP@AL (red), AgNP@ZHL (blue) and in the absence of particles (black) at bactericidal concentrations (concentration B for AgNP@alkali, concentration A for AgNP@AL and AgNP@ZHL according to Table S2†), under dark or light exposure.

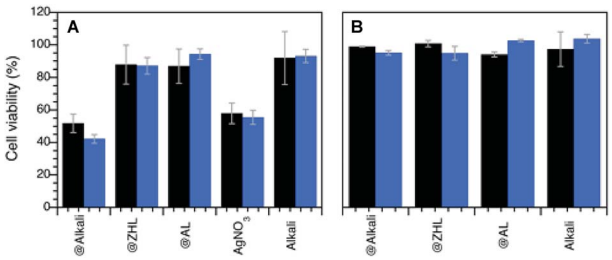

Fig. 6 Cell viability measurements (% relative to cell viability in the absence of nanocomposites) carried out by using MTT colorimetric assay (see Experimental section) of human fibroblasts after (A) 1 h incubation with AgNP@lignin nanocomposites and (B) 6 h incubation with AuNP@lignin at the bactericidal concentrations (concentration B for AgNP@alkali and AuNP@lignin, concentration A for AgNP@ZHL and AgNP@AL, according to Table S2†). Black bars correspond to dark conditions, blue bars under white light irradiation.

could be fully dissolved in the biological media and therefore controls without NP were only run with this type of lignin.

Biofilm eradication

Fig. 7 shows the antimicrobial activity of the AgNP@lignin nanocomposites against *S. aureus* biofilms grown in glucose-rich LB broth. The so-prepared biofilms were subjected to dark and light treatments in the presence of bactericidal concentrations of AgNP@lignin nanocomposites, showing bacteriostatic activity after the incubation time. The biofilm viability (biofilm%) was calculated relative to the control (bacteria in the absence of nanocomposites) using eqn (2):

$$\text{Biofilm}\% = \frac{\text{Abs}_{t_0}^{570} - \text{Abs}_{t_x}^{570}}{\text{Abs}_{t_0}^{570}} \times 100\% \quad (2)$$

where $\text{Abs}_{t_0}^{570}$ is the absorption of the biofilm at time 0 h, before treatment with the nanocomposites, and $\text{Abs}_{t_x}^{570}$ is the absorption of the biofilm in the presence of the nanocomposites at any specific time.

Discussion

Different types of lignins show similar abilities to reduce Ag^+ and Au^{3+} precursors into AgNP or AuNP upon heat or light exposure. As mentioned before, the phenolic groups present in the lignin structure are believed to be responsible for the reducing properties of lignin.[25,26] We noticed the presence of MNP in all the mass ratios explored, however we selected the methodology that furnished to the most stable MNP@lignin in less time. Specifically, alkali lignin shows to be a better reducing and stabilizing agent in the presence of AuNP comparing to AgNP. Despite the fact that the synthesis of AgNP@alkali requires higher metal–lignin mass ratio (5 *versus* 0.5 in the case of AuNP@lignin), the particles show formation of aggregates that can be easily spotted by TEM imaging. We note that ZHL lignin shows the same ability to reduce Ag^+ and Au^{3+}, therefore the same synthetic protocol was selected for both MNP@lignin formation. Finally, AL lignin also shows similar reducing abilities and therefore the synthetic methodologies were selected based on the reaction times. Overall, the reported sugar content on the lignins appears to have no relation to their reducing capacities, although in the case of AgNP it might help preventing particle agglomeration (*cf.* AgNP@alkali with AgNP@ZHL and AgNP@AL).

Overall, the synthesized spherical MNP@lignin nanocomposites are fairly monodisperse as per their TEM images (except in the case of AgNP@alkali), although most of them show some degree of polydispersity according to DLS measurements (PDI > 0.5). According to these measurements the hydrodynamic radii of these nanocomposites are bigger than the particle diameter determined by TEM imaging. This is in agreement with the presence of a bulky lignin-derived shell (Table S2†). The presence of lignin in the nanocomposites was further proved by ATR FT-IR spectroscopy as shown in Fig. S5.† Additionally, the use of lignin as capping agent shows excellent electrostatic stability according to the ζ-potential values found for all the MNP@lignin nanocomposites.[39] Whereas there are many efforts reported to obtained monodisperse and monomorphic NP,[40,41] few reports believe polymorphism and polydispersity could help to avoid bacterial resistance.[42] Therefore, we focused on the good optical properties that all these nanocomposites present, *i.e.* absorption band in the visible region, and also on their stability. The use of NP in clinical settings is usually limited by their aggregation in the biological media, therefore it is important to demonstrate their stability in such environments.[43] Utilizing the stability criterium shown in eqn (1),[17] all MNP@lignin nanocomposites are suitable to be used in different biological media, namely PBS, LB, and DMEM.

Two bacterial strains were chosen to demonstrate the antibacterial activity of MNP@lignin nanocomposites: *S. aureus* and *E. coli*. They are representative for Gram-positive and Gram-negative bacteria, respectively. *S. aureus* is known to present a thicker peptidoglycan layer as oppose to *E. coli*, which contains more fatty acids.[44] From Fig. 4 we can see that the different lignin nanocomposites have different antimicrobial activity. We can recognize the bacteriostatic activity, as less than 3 $\log_{10}$ reduction in CFU, from the bactericidal activity, where the bacterial viability decrease at least 3 $\log_{10}$ in CFU.[45,46] Specifically, under dark conditions AgNP@alkali show bactericidal activity against *E. coli* at the MIC (concentration A, Table S2†) while only bacteriostatic activity is detected at lower

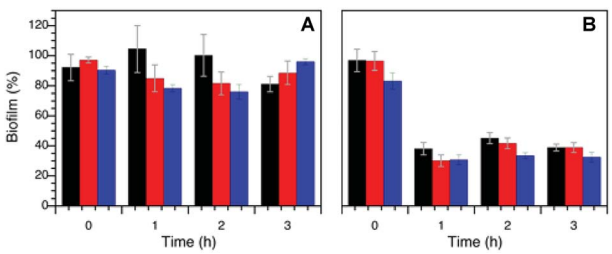

Fig. 7 *S. aureus* biofilm eradication by treatment with AgNP@alkali (black), AgNP@AL (red) and AgNP@ZHL (blue) under dark (A) and under light (B) conditions. (Concentration B for AgNP@alkali, concentration A for AgNP@AL and AgNP@ZHL according to Table S2†).

concentrations (B). In the case of *S. aureus*, the nanocomposites showed bacteriostatic effect under dark conditions at both concentrations (A and B). In all cases, when the nanocomposites are subjected to white light illumination, the antibacterial activity can be recognized by either short exposure times or lower particle concentrations. Similar behavior is found for the AgNP@AL nanocomposites. Interestingly, AgNP@ZHL, show neither bactericidal nor any bacteriostatic activity in the dark at the concentrations studied. However, under illumination they show an increase in activity against *S. aureus* whereas it remains innocuous for *E. coli*. This is a particularly interesting result, as it shows good selectivity towards *S. aureus*. Coincidentally, these nanocomposites contain lignin with higher sugar content, which could contribute to a better interaction with the *S. aureus* bacterial cell wall.[17,47] Additionally, Fig. S9† shows the AuNP@lignin tested are non-toxic for the bacteria in the dark, unless they are subjected to light exposure. Thus, the nanocomposites show bactericidal activity in both strains after 6 hours of irradiation. In comparison to other AuNP studied, such as those coated with sugars[17] or hydrophobic organic ligands,[48] these AuNP@lignin nanocomposites show similar antibacterial concentrations, with the advantage of an easy and rapid synthetic methodology and stability in biological media. Interestingly, all MNP@lignin nanocomposites show better activity under white light irradiation, which potentiates their uses in Photodynamic Antimicrobial Chemotherapy (PACT).[49] It is worth noting that light itself does not produce any damage or change on the normal growth of bacteria.

Interestingly, all nanocomposites studied here are negatively charged according to the ζ-potential measurements (Table 2). Although this can be considered a disadvantage (as bacterial membranes are known to be negatively charged and attracted only by positively charged NP[43,50]), the nanocomposites showed antibacterial activity although we utilized them without further modifications. We believe the sugar content of the lignin could be involved in the adhesion to the bacterial membrane, *i.e.* peptidoglycan layer present in the bacterial cell wall can help to attract sugars, and with them the nanocomposites attached.[17,47]

As mentioned before, there are two main processes that are believed to be involved in the photo-induced antimicrobial activity of MNP,[12,13] namely, photothermal and photochemical mechanisms. The first one involves the absorption of light by the MNP and the concomitant local release of heat from the particle that can destroy biomolecules (or melt the lipids in a cell membrane) in close proximity to the MNP surface.[51] The photochemical mechanism implicates the production of ROS by electron transfer processes from MNP to oxygen in the media. The later can be determined by a simple measurement of ROS generated during irradiation process. Fig. 5 shows how the generation of ROS is increased 2-fold when the nanocomposites are expose to visible light. The maximum ROS production enhancement in the presence of AgNP@alkali and AgNP@AL nanocomposites occurs after 10 min of irradiation. Subsequently, due to the bacteria being killed (*cf.* Fig. 4), the production of ROS cannot be further identified by this methodology. Additionally, AgNP@ZHL do not show ROS production increase upon irradiation compared to the control, which is in agreement with the absence of antibacterial activity under dark conditions. This result proves that the main mechanism of action for this nanocomposite does not involve a photochemical process. In the case of AuNP@lignin nanocomposites only solutions of concentration B increase the production of ROS above the control level, this is probably related to a lower concentration of lignin and the concomitant decrease of its antioxidant effect.

Fibroblasts are very sensitive to external factors, as opposed to HeLa cells – most frequently used for *in vitro* experiments –, and therefore more relevant for the analysis of the effects of new drugs on eukaryotic cells.

None of the MNP@lignin nanocomposites have shown cytotoxic effects, except for the AgNP@alkali. Although this composite acts as better antimicrobial agents than $AgNO_3$, they can be equally toxic. We believe that a synergistic effect due to the presence of both the big agglomerates (that can improve antimicrobial activity), and the small NPs (that can release high amount of silver ions involved in the increase of cytotoxicity) can explain the activity of this composite.[52–54] We attribute this effect to the type of lignin used (alkali), which is not as strong a stabilizer for AgNP as the other lignin studied here.

Finally, and yet importantly, the formation of biofilms is a growing concern as the encapsulation of bacterial cells in the film plays an important role on their persistency and decreases their vulnerability to antimicrobials.[55] This can make them not only more dangerous but also more difficult to eliminate.[56] In particular, *S. aureus* biofilms cause many infections[57] and their eradication is essential.[58] Towards this goal, we decided to test the antimicrobial activity of AgNP@lignin nanocomposites to eliminate *S. aureus* biofilms upon white light irradiation. All nanocomposites show great activity, where over 60% of the biofilm was eliminated after one hour of irradiation (Fig. 7).

Conclusions

The use of natural compounds, that can find value-added application while being eco-friendly materials, is important not only to favour sustainable practices but also to protect the environment. Here we show that MNP@lignin nanocomposites could be synthesized with a simple one-step method under very mild conditions that can involve heat or visible light. The nanocomposites are stable for more than a week in different biological media, keeping their optical properties and being persistently well-dispersed in the media. The nature of the lignin drastically alters the antibacterial properties of the nanocomposites; it is believed the interaction of the nanocomposites with the bacterial cell wall can be governed by the lignin structure helping not only on the stability of the particles but also on their selectivity towards different type of bacteria. Finally the nanocomposites are non-toxic and show great potential to act as bacteriostatic agents against biofilms.

Conflicts of interest

There are no conflicts to declare.

Acknowledgements

This work was supported by the Natural Sciences and Engineering Research Council of Canada, the Canada Foundation for Innovation, and the Canada Research Chairs Program. D. R. and J. P. V. were grateful recipients of the Emerging Leaders of the Americas Program from Canada. D. M. R. is supported by the SECyT UNC fellowship (Argentina). M. C. B. is member of the Research career of CONICET.

References

1 WHO, *Antimicrobial resistance: global report on surveillance 2014*, 2014, p. 257.
2 K. Yang, Q. Han, B. Chen, Y. Zheng, K. Zhang, Q. Li and J. Wang, Antimicrobial hydrogels: promising materials for medical application, *Int. J. Nanomed.*, 2018, **13**, 2217.
3 T. Ellis, M. Chiappi, A. García-Trenco, M. Al-Ejji, S. Sarkar, T. K. Georgiou, M. S. P. Shaffer, T. D. Tetley, S. Schwander, M. P. Ryan and A. E. Porter, Multimetallic Microparticles Increase the Potency of Rifampicin against Intracellular Mycobacterium tuberculosis, *ACS Nano*, 2018, **12**, 5228.
4 J. R. Koduru, S. K. Kailasa, J. R. Bhamore, K.-H. Kim, T. Dutta and K. Vellingiri, Phytochemical-assisted synthetic approaches for silver nanoparticles antimicrobial applications: a review, *Adv. Colloid Interface Sci.*, 2018, **256**, 326.
5 A. Patir, G. B. Hwang, S. P. Nair, E. Allan and I. P. Parkin, Photobactericidal Activity of Dual Dyes Encapsulated in Silicone Enhanced by Silver Nanoparticles, *ACS Omega*, 2018, **3**, 6779.
6 Y. Qiao, F. Ma, C. Liu, B. Zhou, Q. Wei, W. Li, D. Zhong, Y. Li and M. Zhou, Near-Infrared Laser-Excited Nanoparticles To Eradicate Multidrug-Resistant Bacteria and Promote Wound Healing, *ACS Appl. Mater. Interfaces*, 2018, **10**, 193.
7 Z. M. Xiu, Q. B. Zhang, H. L. Puppala, V. L. Colvin and P. J. J. Alvarez, Negligible Particle-Specific Antibacterial Activity of Silver Nanoparticles, *Nano Lett.*, 2012, **12**, 4271.
8 E. I. Alarcon, K. Udekwu, M. Skog, N. L. Pacioni, K. G. Stamplecoskie, M. Gonzalez-Bejar, N. Polisetti, A. Wickham, A. Richter-Dahlfors, M. Griffith and J. C. Scaiano, The biocompatibility and antibacterial properties of collagen-stabilized, photochemically prepared silver nanoparticles, *Biomaterials*, 2012, **33**, 4947.
9 K. K. Comfort, E. I. Maurer, L. K. Braydich-Stolle and S. M. Hussain, Interference of silver, gold, and iron oxide nanoparticles on epidermal growth factor signal transduction in epithelial cells, *ACS Nano*, 2011, **5**, 10000.
10 R. M. Dragoman, M. Grogg, M. I. Bodnarchuk, P. Tiefenboeck, D. Hilvert, D. N. Dirin and M. V. Kovalenko, Surface-Engineered Cationic Nanocrystals Stable in Biological Buffers and High Ionic Strength Solutions, *Chem. Mater.*, 2017, **29**, 9416.
11 C. M. J. Silvero, D. M. Rocca, E. A. de la Villarmois, K. Fournier, A. E. Lanterna, M. F. Perez, M. C. Becerra and J. C. Scaiano, Selective Photoinduced Antibacterial Activity of Amoxicillin-Coated Gold Nanoparticles: From One-Step Synthesis to *in Vivo* Cytocompatibility, *ACS Omega*, 2018, **3**, 1220.
12 A. P. Castano, T. N. Demidova and M. R. Hamblin, Mechanisms in photodynamic therapy: part one-photosensitizers, photochemistry and cellular localization, *Photodiagn. Photodyn. Ther.*, 2004, **1**, 279.
13 X. H. Huang, I. H. El-Sayed, W. Qian and M. A. El-Sayed, Cancer cell imaging and photothermal therapy in the near-infrared region by using gold nanorods, *J. Am. Chem. Soc.*, 2006, **128**, 2115.
14 T. T. Tsai, T. H. Huang, C. J. Chang, N. Y. J. Ho, Y. T. Tseng and C. F. Chen, Antibacterial cellulose paper made with silver-coated gold nanoparticles, *Sci. Rep.*, 2017, **7**, 3155.
15 M. Sathiyabama and A. Manikandan, Application of Copper-Chitosan Nanoparticles Stimulate Growth and Induce Resistance in Finger Millet (Eleusine coracana Gaertn.) Plants against Blast Disease, *J. Agric. Food Chem.*, 2018, **66**, 1784.
16 J. H. Johnston and T. Nilsson, Nanogold and nanosilver composites with lignin-containing cellulose fibres, *J. Mater. Sci.*, 2012, **47**, 1103.
17 H. D. Weerasekera, M. J. Silvero, D. R. C. da Silva and J. C. Scaiano, A database on the stability of silver and gold nanostructures for applications in biology and biomolecular sciences, *Biomater. Sci.*, 2017, **5**, 89.
18 D. Kai, M. J. Tan, P. L. Chee, Y. K. Chua, Y. L. Yap and X. J. Loh, Towards lignin-based functional materials in a sustainable world, *Green Chem.*, 2016, **18**, 1175.
19 L. W. Mu, J. Wu, L. Matsakas, M. J. Chen, A. Vahidi, M. Grahn, U. Rova, P. Christakopoulos, J. H. Zhu and Y. J. Shi, Lignin from Hardwood and Softwood Biomass as a Lubricating Additive to Ethylene Glycol, *Molecules*, 2018, **23**, 537.
20 J. Berghel, S. Frodeson, K. Granstrom, R. Renstrom, M. Stahl, D. Nordgren and P. Tomani, The effects of kraft lignin additives on wood fuel pellet quality, energy use and shelf life, *Fuel Process. Technol.*, 2013, **112**, 64.
21 W. J. Yang, E. Fortunati, D. Q. Gao, G. M. Balestra, G. Giovanale, X. Y. He, L. Torre, J. M. Kenny and D. Puglia, Valorization of Acid Isolated High Yield Lignin Nanoparticles as Innovative Antioxidant/Antimicrobial Organic Materials, *ACS Sustainable Chem. Eng.*, 2018, **6**, 3502.
22 Z. G. Shen, Y. Q. Luo, Q. Wang, X. Y. Wang and R. C. Sun, High-Value Utilization of Lignin to Synthesize Ag Nanoparticles with Detection Capacity For Hg^{2+}, *ACS Appl. Mater. Interfaces*, 2014, **6**, 16147.
23 K. R. Aadil, A. Barapatre, A. S. Meena and H. Jha, Hydrogen peroxide sensing and cytotoxicity activity of Acacia lignin stabilized silver nanoparticles, *Int. J. Biol. Macromol.*, 2016, **82**, 39.
24 Y. Polat; E. Stojanovska; T. A. Negawo; E. Doner; A. Kilic in *Green Biocomposites: Manufacturing and Properties*, ed. M.Jawaid, S. M.Sapuan, O. Y.Alothman, Springer International Publishing, Cham, 2017; p. 71.
25 M. J. Rak, T. Friscic and A. Moores, Mechanochemical synthesis of Au, Pd, Ru and Re nanoparticles with lignin as

a bio-based reducing agent and stabilizing matrix, *Faraday Discuss.*, 2014, **170**, 155.
26 K. R. Aadil, A. Barapatre, S. Sahu, H. Jha and B. N. Tiwary, Free radical scavenging activity and reducing power of Acacia nilotica wood lignin, *Int. J. Biol. Macromol.*, 2014, **67**, 220.
27 M. B. Marulasiddeshwara, S. S. Dakshayani, M. N. Sharath Kumar, R. Chethana, P. Raghavendra Kumar and S. Devaraja, Facile-one pot-green synthesis, antibacterial, antifungal, antioxidant and antiplatelet activities of lignin capped silver nanoparticles: a promising therapeutic agent, *Mater. Sci. Eng., C*, 2017, **81**, 182.
28 A. P. Richter, J. S. Brown, B. Bharti, A. Wang, S. Gangwal, K. Houck, E. A. C. Hubal, V. N. Paunov, S. D. Stoyanov and O. D. Velev, An environmentally benign antimicrobial nanoparticle based on a silver-infused lignin core, *Nat. Nanotechnol.*, 2015, **10**, 817.
29 P. Zhang, S. Li, H. Chen, X. Wang, L. Liu, F. Lv and S. Wang, Biofilm Inhibition and Elimination Regulated by Cationic Conjugated Polymers, *ACS Appl. Mater. Interfaces*, 2017, **9**, 16933.
30 N. L. Pacioni, M. Gonzalez-Bejar, E. Alarcon, K. L. McGilvray and J. C. Scaiano, Surface Plasmons Control the Dynamics of Excited Triplet States in the Presence of Gold Nanoparticles, *J. Am. Chem. Soc.*, 2010, **132**, 6298.
31 I. Tamosiune, G. Staniene, P. Haimi, V. Stanys, R. Rugienius and D. Baniulis, Endophytic Bacillus and Pseudomonas spp. Modulate Apple Shoot Growth, Cellular Redox Balance, and Protein Expression Under *in Vitro* Conditions, *Front. Plant Sci.*, 2018, **9**, 889.
32 E. A. Trafny, R. Lewandowski, I. Zawistowska-Marciniak and M. Stepinska, Use of MTT assay for determination of the biofilm formation capacity of microorganisms in metalworking fluids, *World J. Microbiol. Biotechnol.*, 2013, **29**, 1635.
33 K. G. Stamplecoskie and J. C. Scaiano, Light Emitting Diode Irradiation Can Control the Morphology and Optical Properties of Silver Nanoparticles, *J. Am. Chem. Soc.*, 2010, **132**, 1825.
34 A. Lanterna, E. Pino, A. Domenech-Carbo, M. Gonzalez-Bejar and J. Perez-Prieto, Enhanced catalytic electrochemical reduction of dissolved oxygen with ultraclean cucurbituril [7]-capped gold nanoparticles, *Nanoscale*, 2014, **6**, 9550.
35 Malvern Dynamic light scattering common terms defined. http://www.biophysics.bioc.cam.ac.uk/wp-content/uploads/2011/02/DLS_Terms_defined_Malvern.pdf (accessed 2018-11-08).
36 M. B. Marulasiddeshwara, S. S. Dakshayani, M. N. S. Kumar, R. Chethana, P. R. Kumar and S. Devaraja, Facile-one pot-green synthesis, antibacterial, antifungal, antioxidant and antiplatelet activities of lignin capped silver nanoparticles: a promising therapeutic agent, *Mater. Sci. Eng., C*, 2017, **81**, 182.
37 B. Mai, Y. Gao, M. Li, X. Wang, K. Zhang, Q. Liu, C. Xu and P. Wang, Photodynamic antimicrobial chemotherapy for Staphylococcus aureus and multidrug-resistant bacterial burn infection *in vitro* and *in vivo*, *Int. J. Nanomed.*, 2017, **12**, 5915.
38 S. Sabella, R. P. Carney, V. Brunetti, M. A. Malvindi, N. Al-Juffali, G. Vecchio, S. M. Janes, O. M. Bakr, R. Cingolani, F. Stellacci and P. P. Pompa, A general mechanism for intracellular toxicity of metal-containing nanoparticles, *Nanoscale*, 2014, **6**, 7052.
39 S. Bhattacharjee, DLS and zeta potential - What they are and what they are not?, *J. Controlled Release*, 2016, **235**, 337.
40 D. Rioux and M. Meunier, Seeded Growth Synthesis of Composition and Size-Controlled Gold–Silver Alloy Nanoparticles, *J. Phys. Chem. C*, 2015, **119**, 13160.
41 K. L. McGilvray, C. Fasciani, C. J. Bueno-Alejo, R. Schwartz-Narbonne and J. C. Scaiano, Photochemical strategies for the seed-mediated growth of gold and gold-silver nanoparticles, *Langmuir*, 2012, **28**, 16148.
42 S. Veeraapandian, S. N. Sawant and M. Doble, Antibacterial and antioxidant activity of protein capped silver and gold nanoparticles synthesized with Escherichia coli, *J. Biomed. Nanotechnol.*, 2012, **8**, 140.
43 L. L. Wang, C. Hu and L. Q. Shao, The antimicrobial activity of nanoparticles: present situation and prospects for the future, *Int. J. Nanomed.*, 2017, **12**, 1227.
44 W. Wang, Y. Zhu and X. Chen, Selective Imaging of Gram-Negative and Gram-Positive Microbiotas in the Mouse Gut, *Biochemistry*, 2017, **56**, 3889.
45 G. A. Pankey and L. D. Sabath, Clinical relevance of bacteriostatic *versus* bactericidal mechanisms of action in the treatment of Gram-positive bacterial infections, *Clin. Infect. Dis.*, 2004, **38**, 864.
46 F. Ghilini, R. C. R. Gonzalez, A. G. Minan, D. Pissinis, A. H. Creus, R. C. Salvarezza and P. L. Schilardi, Highly Stabilized Nanoparticles on Poly-L-Lysine-Coated Oxidized Metals: A Versatile Platform with Enhanced Antimicrobial Activity, *ACS Appl. Mater. Interfaces*, 2018, **10**, 23657.
47 T. T. Le, R. P. Pandey, R. B. Gurung, D. Dhakal and J. K. Sohng, Efficient enzymatic systems for synthesis of novel alpha-mangostin glycosides exhibiting antibacterial activity against Gram-positive bacteria, *Appl. Microbiol. Biotechnol.*, 2014, **98**, 8527.
48 X. N. Li, S. M. Robinson, A. Gupta, K. Saha, Z. W. Jiang, D. F. Moyano, A. Sahar, M. A. Riley and V. M. Rotello, Functional Gold Nanoparticles as Potent Antimicrobial Agents against Multi-Drug-Resistant Bacteria, *ACS Nano*, 2014, **8**, 10682.
49 C. Fasciani, M. J. Silvero, M. A. Anghel, G. A. Arguello, M. C. Becerra and J. C. Scaiano, Aspartame-stabilized gold-silver bimetallic biocompatible nanostructures with plasmonic photothermal properties, antibacterial activity, and long-term stability, *J. Am. Chem. Soc.*, 2014, **136**, 17394.
50 Y. N. Slavin, J. Asnis, U. O. Hafeli and H. Bach, Metal nanoparticles: understanding the mechanisms behind antibacterial activity, *J. Nanobiotechnol.*, 2017, **15**, 65.
51 G. Palermo, D. Pagnotto, L. Ricciardi, L. Pezzi, M. La Deda and A. De Luca, Thermoplasmonic Effects in Gain-Assisted Nanoparticle Solutions, *J. Phys. Chem. C*, 2017, **121**, 24185.

52 C. Levard, E. M. Hotze, G. V. Lowry and G. E. Jr Brown, Environmental transformations of silver nanoparticles: impact on stability and toxicity, *Environ. Sci. Technol.*, 2012, **46**, 6900.

53 A. D'Agostino, A. Taglietti, P. Grisoli, G. Dacarro, L. Cucca, M. Patrini and P. Pallavicini, Seed mediated growth of silver nanoplates on glass: exploiting the bimodal antibacterial effect by near IR photo-thermal action and Ag^{+} release, *RSC Adv.*, 2016, **6**, 70414.

54 A. D'Agostino, A. Taglietti, R. Desando, M. Bini, M. Patrini, G. Dacarro, L. Cucca, P. Pallavicini and P. Grisoli, Bulk Surfaces Coated with Triangular Silver Nanoplates: Antibacterial Action Based on Silver Release and Photo-Thermal Effect, *Nanomaterials*, 2017, **7**, 7.

55 H. Wolfmeier, D. Pletzer, S. C. Mansour and R. E. W. Hancock, New Perspectives in Biofilm Eradication, *ACS Infect. Dis.*, 2018, **4**, 93.

56 M. Sadekuzzaman, S. Yang, M. F. R. Mizan and S. D. Ha, Current and Recent Advanced Strategies for Combating Biofilms, *Compr. Rev. Food Sci. Food Saf.*, 2015, **14**, 491.

57 C. Kong, C. F. Chee, K. Richter, N. Thomas, N. Abd Rahman and S. Nathan, Suppression of Staphylococcus aureus biofilm formation and virulence by a benzimidazole derivative, UM-C162, *Sci. Rep.*, 2018, **8**, 2758.

58 J. L. Lister and A. R. Horswill, Staphylococcus aureus biofilms: recent developments in biofilm dispersal, *Front. Cell. Infect. Microbiol.*, 2014, **4**, 178.